Gondwana break-up controlled by tectonic inheritance and mantle plume activity: insights from Natal rift development (South Mozambique, Africa)

Vincent Roche, Sylvie Leroy, Sidonie Révillon, François Guillocheau, Gilles Ruffet, W. Vétel

LEROY Sylvie (Orcid ID: 0000-0002-3188-8802)

Gondwana break-up controlled by tectonic inheritance and mantle plume activity: insights from Natal rift development (South Mozambique, Africa)

Roche V.[1], Leroy S.[1], Revillon, S.[2], Guillocheau, F.[3], Ruffet, G.[3], Vétel, W.[4]

[1] Sorbonne Université, CNRS, Institut des Sciences de la Terre de Paris, ISTeP, Paris, France

[2] Sedisor/LGO-IUEM, Brest, France

[3] Univ Rennes, CNRS, Géosciences Rennes, UMR 6118, 35000 Rennes France

[4] TotalEnergies Exploration et Production, Pau, France

@ vincent.roche@sorbonne-universite.fr

This article has been accepted for publication and undergone full peer review but has not been through the copyediting, typesetting, pagination and proofreading process which may lead to differences between this version and the Version of Record. Please cite this article as doi: 10.1111/ter.12590

KEY POINTS:

- The Natal magma-rich segment is characterized by seaward dipping reflectors corresponding to large volume of basalts
- Isotope data suggest that basaltic samples from wells were generated through melting of similar primitive mantle reservoir
- Tectonic inheritance favors extension and upwelling from a deep mantle thermomechanical anomaly
- The oceanic seafloor spreading of the Natal oceanic basin should have occurred at ca. 160 Ma at 30°S

ABSTRACT

The breakup of Eastern Gondwana started during the Early Jurassic with the separation of Antarctica and Madagascar from Africa. While margins architecture has been described along the Western Somalia Basin and the central Mozambique, the spatial extent of rifting further south – *i.e.* the Natal Valley – remains poorly documented. Seismic reflection profiles interpretation, $^{40}Ar/^{39}Ar$ ages and isotopic data show the existence of a plume related magma-rich margin – the Natal segment – characterized by a large volume of seaward dipping reflectors inferred to be basalts. In particular, the contrast in lithosphere rheology, probably caused by a Meso-Neoproterozoic belt between the Kaapval and Grunehogna Archean cratons, favored extension and upwelling from a deep mantle thermomechanical anomaly, the so-called Karoo superplume that started at around 180 Ma. Further, the presence of stretched continental crust at around 30°S implies a more southerly position of Antarctica which will need to be considered in future kinematic models.

1. INTRODUCTION

The Mozambique oblique magma-rich passive margin (SE offshore Africa, Fig. 1a) related to the breakup of Gondwana, is constituted by three distinct segments, (i) the Angoche, (ii) the Beira-High, and (iii) the Natal segments (Fig. 1b), separated by major fractures zones (FZ). The complexity of this margin is mainly caused by pre-existing structures with contrast trends (*e.g.*, NE-SW and N-S, Mahanjane, 2012; Senkans *et al*., 2019; Roche *et al*., 2021) and by a long-lived magmatic activity from *ca.* 180 Ma to the present (Fig. 2) (*e.g.*, Jourdan *et al*., 2007a; Mueller & Jokat, 2017; Senkans *et al*., 2019; Watremez *et al*., 2021).

It is generally assumed that the Jurassic extension along the Mozambique margins results from mantle plume activity (*e.g.*, Cox, 1992; White 1997; Storey & Kyle, 1997; Roche *et al*., 2021). However, based on structural features (Watkeys, 2002; Klausen, 2009; Hastie *et al*., 2014), and geochemical and geochronological data (Jourdan *et al*., 2006; Jourdan *et al*., 2007b), a number of studies explained the large volumes of extrusive basalts by tectonic crustal thinning. At the regional-scale, the basalts formed the large igneous province (LIP) at ca. 180 Ma (Jourdan *et al*., 2007a), dike swarms interpreted as a failed branch of a rift (White & McKenzie, 1989; Watkeys, 2002), lava delta (Roche *et al*., 2021) and sills recognized in seaward dipping reflectors (SDRs) (*e.g.*, Watkeys, 2002; Riley *et al*. 2004; Mueller & Jokat, 2017, 2019; Senkans *et al*., 2019). These events were followed by NW-SE oceanic spreading from *ca.* 164 Ma to *ca.* 156 Ma, depending on the considered segment (Beira High being younger than Angoche segment) and the interpretation (*e.g.,* Mahanjane, 2012; Senkans *et al*., 2019; Mueller & Jokat, 2019). Subsequently, a clockwise rotation of the regional stress-field to N-S, related to the southward drift of Madagascar and Antarctic plates relative to the African plate (*e.g.*, Cox, 1992; König & Jokat, 2006; Leinweber & Jokat, 2012; Bhattacharya & Duval, 2016; Klimke *et al*., 2018; Mueller & Jokat, 2019) formed ENE-WSW oriented magnetic anomalies

and main transform segments (*e.g.*, the Davie FZ - Roche and Ringenbach, 2021 and the Mozambique FZ - Limpopo FZ - Roche *et al*., 2021). Although the Mozambique Basin is known to follow this evolution, there is no consensus on plate reconstructions (Eagles & König, 2008; König & Jokat, 2010; Leinweber & Jokat, 2012; Thompson *et al*., 2019; Mueller & Jokat, 2019) which depend mainly on the interpretation of the nature of the crust in different places (*i.e.*, oceanic vs. continental) (Fig. 1b).

The Natal Valley (south Mozambique) is the key segment to address this question (Fig. 1b). It is bounded by the Mozambique FZ and the Limpopo FZ (Roche *et al*., 2021) to the east and by the Jurassic Karoo volcanic rocks of the Lebombo Monocline to the west (Fig. 1b). The crust in the north of the Natal Valley (Zululand basin, Fig. 1b) has been variously interpreted as continental and/or transitional (*e.g.*, Dingle & Scrutton, 1974; Raillard, 1990; Goodlag, 1986; Hanyu *et al*., 2017) or oceanic (*e.g.*, Green, 1972; Tikku *et al*., 2002; Leinweber & Jokat, 2011). Recent P-waves refraction models show a 30 km-thick continental crust with possible magmatic underplating below the Zululand basin and a rapid thinning of the crust toward the south (20 km in 60 km, Moulin *et al*. 2020; Leprêtre *et al*., 2021). In addition to structural domains characterization, the style of deformation and the influence of magmatism related to the Early Jurassic Karoo event described along the Lebombo Monocline have yet to be investigated.

Offshore seismic reflection profiles combined with $^{40}Ar/^{39}Ar$ ages and isotopic data from wells enable us to discuss for the first time the structural and volcanic character of the Natal segment compared with the mantle plume activity. These new elements provide major constraints on plate tectonic reconstructions.

2. DATA AND METHODS

2.1. Seismic data set and stratigraphy

Our seismic data set consists of different seismic surveys available at TotalEnergies, merged with seismic refraction profiles from the PAMELA-MOZ3/5 cruise on the R/V Pourquoi Pas? (Moulin *et al*., 2016a, 2016b; Watremez *et al*., 2021). In particular, we used the CGG 2D seismic survey which contains 42 lines spaced over the Durban and Zululand Basins (see Bhattacharya and Duval, 2016) to present a new map of sub-crustal domains. Crustal thickness maps from Hanyu *et al*. (2017) (Fig. 2a) derived from marine gravity data from Sandwell and Smith (2009) jointly with magnetic data have also been combined to define the major crustal domains, including a magmatic continental domain (thick and thinned), a transitional domain made of SDRs and the magmatic oceanic domain (Fig. 2b).

We present here two simplified cross-sections based on multichannel seismic reflection profiles to characterize the margin crustal architecture (see Fig. 2a for location). Seismic profiles interpretations were carried out in time-domain. Particular attention has been paid to the thick volcanic packages imaged at depth below the acoustic basement defined by various sets of reflectors. The base of sediments is picked as a volcanic erosional surface which corresponds to the top unit 1 (TU1) and the top volcanics (TU2 to TU4). TU1 may tentatively be attributed to the Early Jurassic (Flores, 1984; Raillard, 1990; Salman & Abdula, 1995) whereas others have unknown ages. In order to confirm this age, we collected mafic whole-rock fragments from the Zululand well and we applied the $^{40}Ar/^{39}Ar$ method detailed in the Supplementary Material. This well is located on the proximal margin in the onshore domain (Fig. 2a). Other wells available at TotalEnergies have been used to constrain markers and seismic facies (Fig. 2a). Interestingly, the northern part of the continental margin (the Mozambique Coastal Plain, MCP) recorded a significant tectonic and sedimentary hiatus during the margin evolution from the Early Jurassic to Valanginian (*e.g.*, Flores, 1984; Roche *et al*., 2021).

2.2. Isotopic data

We analyzed a subset of 20 mainly basaltic samples from four wells for Sr, Nd and Pb isotopes located along the Lebombo Monocline, in the MCP and northeast of the MCP along the Beira High segment (Fig. 1b). All samples analyzed are located at the bottom of the wells below Valanginian sediments. Fractions were chemically separated following conventional column chemistry procedures described in Revillon *et al*. (2011) and Gale (1996). Sr and Pb isotope compositions were measured in static mode on a Thermo TRITON and a Neptune Multi-collector Inductively Coupled Plasma Mass Spectrometer at the PSO (Pôle de Spectrométrie Océan) in Brest, France. All measured Sr and Nd ratios were normalized to $^{86}Sr/^{88}Sr = 0.1194$ and $^{146}Nd/^{144}Nd = 0.7219$ respectively. During the course of analysis, Sr isotope compositions of standard solution NBS987 gave $^{87}Sr/^{86}Sr = 0.710267 \pm 0.000008$ (2σ) (n=7, recommended value 0.710250). Pb isotope ratios were corrected for instrumental mass fractionation and machine bias by the Tl doping method of White *et al*. (2000) and SRM981 Pb standard bracketing every 3 samples. Pb isotope reproducibility, based on 16 replicate analyses of NIST SRM981 is 0.0008 (2 σ) for $^{206}Pb/^{204}Pb$ and $^{207}Pb/^{204}Pb$ and 0.0023 (2 σ) for $^{208}Pb/^{204}Pb$.

3. RESULTS

3.1. Seismic observations and interpretations

Figure 3 shows a simplified NNW-SSE cross-section based mainly on our seismic observations (MZ7 seismic profile). In detail, this section can be subdivided into three distinct structural sub-

domains (Fig. 3a). In the proximal domain, the top of unit 1 (TU1) is quasi-horizontal under a thin sedimentary cover of 1 s TWTT (2 km) to the north which decreases progressively southward (Figs. 3b and 3c). Below, seismic reflectors R1 are observed. They are characterized by a set of 10 to 20 km-long bright and coherent reflectors. They have medium amplitudes and low to medium frequencies. Interestingly, rocks dated from Zululand (Fig. 4) and from Funhalouro (Roche *et al*., 2021) wells belong to this seismic unit according to our seismic interpretation (Fig. 3a). Such a correlation implies a volcanic affinity for R1. This is also consistent with the observed seismic pattern showing similar characteristics of large lava flows or interstratified volcanoclastics and lava flows (*e.g.*, Planke *et al*., 2000). This domain underwent modest stretching compared to the south. The necking domain is wide and it contains various groups of R2 reflectors bounded by TU1, TU2a, and TU2b (Figs. 3c and 3d). Below these horizons, reflectors R2 are characterized by bright and coherent reflectors with medium amplitudes and medium frequency, onlapping onto basement highs (*e.g.*, Fig. 3d). These groups of reflectors are interpreted as magmatic volcanic series dipping toward the southeast. They show a remarkable divergent geometrical pattern guided by a series of high-angle normal faults (Figs. 3b and 3d). We, therefore, consider them as inner SDRs following the primary definition of SDRs (Planke, 1994; Planke *et al*., 2000). They are limited southwards by an outer magmatic high – the Naude Ridge – which is characterized here by a fairly strong top reflection and chaotic internal reflection (see the mound in Fig. 3b). To the south of this structural high, a thick basin (around 2 s TWTT, Durban Basin in Fig. 3a) covers the relatively flat TU3c. TU3a is disturbed by many E-W trending faults witnessing normal to transtensional movement during the Cretaceous (Fig. 3d). Here, several sub-units are again recognized (Figs. 3b and 3e), but the wedge geometries are not controlled by faults (Fig. 3e). Similar to R2 reflectors, reflections R3 are strong, continuous, smooth and onlap is often observed (Fig. 3d). They are interpreted as

lava flows corresponding to the outer SDR sequences belonging to the magmatic domain (Fig. 3e).

Figure 5 shows a simplified WNW-ESE cross-section based on our seismic observations, and the recent observations of Li *et al*. (2021). The section can be subdivided into four distinct domains, from west to east. The first one corresponds to the proximal domain, which is characterized by two different groups of reflectors R1 and R0 (Fig. 5b), separated by a major unconformity. As previously mentioned, R1 have a volcanic affinity yielding an Early Jurassic age (Fig. 4). Below this unit, R0 are characterized by a set of transparent to low amplitude reflectors, showing wedge-shaped geometries with probable onlaps onto a westward basement high (Fig. 5b). We suggest that U0 is mainly composed of sediments but magmatic addition cannot be totally excluded. This seismic package is only observed to the west reaching several kilometers of thickness close to the normal fault (Fig. 5b), and cannot be totally excluded in the eastern part of the section. TU1 appears to be quasi horizontal in its western part, and it is locally cross-cut by Cretaceous faults showing mainly a normal to transtensional component (Fig. 5a). The necking domain related to the Natal rifted margin (domain-a) shows similar features as the previous cross-section. Below post-rift sediments, various groups of seismic reflectors (R2) are identified overlapping progressively westwards (Fig. 5c), parallel to the TU1 (Fig. 5a). R2 are characterized here by inclined and alternating strong and weak reflectors (Li *et al*., 2021), and correspond to SDRs in our interpretation. The third domain corresponds to a secondary long necking domain (90 – 100 km, domain-b in Fig. 5a), which is characterized by a strong thinning of the crust. This thinning seems to be accommodated on high angle strike-slip faults and strongly intruded by multiple magmatic features (*e.g.*, dikes, sills) (Fig. 5c). The seismic pattern here is characterized by westward-dipping reflectors controlled by a major fault and by discontinuous dipping reflectors. This unit shows again seismic patterns similar to R2 and R3, and may therefore correspond to volcanic layers. But, they are observed within the Limpopo

FZ. Finally, the last domain corresponds to the oceanic domain. It is bounded westward by the major escarpment related to faulting (Fig. 5c).

Our interpretations of seismic data combined with well dating and regional structural analyzes allow us to revise the previously proposed limits and we present a new map of sub-crustal domains along the Natal Valley with regards to the Mozambique continental margins. According to previous geophysical interpretations (Hanyu *et al*., 2017; Moulin *et al*., 2020; Leprêtre *et al*., 2021) and the presence of large inner SDRs over a thinned crust, the continental domain extending up to 30°S latitude is bounded by the Limpopo FZ to the east and close to the northern termination of the Weddell Sea to the west (Fig. 2b). The southern part of the necking zone (*i.e.*, the Naude Ridge which corresponds to the distal necking, Fig. 3a) consists of outer SDRs implying that the crust below is rich to entirely magmatic. This is consistent with P-waves velocities (Moulin *et al*., 2020; Leprêtre *et al*., 2021). Interestingly, a piece of continental crust extends southwards along the Mozambique Ridge. The presence of continental rocks within the DSDP 249 and the intensity of magnetization like the northern Natal Valley (Hanyu *et al*., 2017) tend to support a continental affinity.

3.2. Isotopic interpretation

The radiogenic isotope compositions of our samples undoubtedly confirm that the basalts and associated volcanic rocks have erupted in a Continental Flood Basalt (CFB) (Fig. 6). Indeed, samples from three wells (Zululand, Funhalouro and Nhachengue) plot very close to the field defined by the Siberian CFB. It should also be noticed that Zululand and Funhalouro samples are very close to the Rooi Rand Dyke complex composition which is characteristics of the Karoo LIP (Jourdan *et al.,* 2007a). In addition, these samples yield an Early Jurassic age (Fig. 4; see Roche *et al*. (2021) for the Funhalouro well). Samples from Nhachengue well, although

very close geographically to Funhalouro well, display higher $^{206}Pb/^{204}Pb$ at an almost constant $^{87}Sr/^{86}Sr$ ratio, indicating either melting of a more enriched mantle source such as the EM2 mantle type or some contamination of magma *en route* to the surface by upper continental crust (Fig. 6). On the other hand, samples from Nhamura well display both higher $^{207}Pb/^{204}Pb$ and $^{87}Sr/^{86}Sr$ at a constant $^{206}Pb/^{204}Pb$ likely indicating that another source, more likely another continental lithospheric mantle or crust, was involved in the generation of the magma. Anyhow, whatever process is invoked to explain the formation of these magmas, it appears that volcanics from the Lebombo Monocline and the MCP are compositionally different from those from Nhamura which is located northeastward. It can therefore be suggested that these two sets of samples are affected by a different type of crustal component during their formation. Such an idea is also supported by the study of Turunen *et al*. (2019) showing geochemical similarities between picrites located north of Nhamura well and the Karoo flood basalts.

4. DISCUSSION

4.1. Tectonic activity during the break-up of Gondwana

The first set of faults – *i.e.* the N-S trending – is located along the Mozambique coast and may extend onshore with the eastward dipping lava flows reported by Riley *et al*. (2004) along the central part of the Lebombo Monocline. This lava wedge controlled by N-S trending faults is dated at *ca.* 180 Ma (our new argon ages; Jourdan *et al*., 2007a) and thus corresponds to the Karoo LIP. The negative gravity anomaly located in the same area (see Leinweber & Jokat, 2011) may also constrain the extension of the regional N-S trending half grabens system filled by Early Jurassic volcanic rocks. The second set of faults – *i.e.* the NE-SW trending set – is

also associated with volcanic wedges. These inner magmatic SDRs are likely linked with Early Jurassic extension and develop during the thinning of the crust by faulting of the upper brittle crust. This is also consistent with the crustal distribution of the magnetization showing both normal and reversed polarity periods (Hanyu *et al*., 2017), implying also a multistage magmatic activity through this time. Thus, it is assumed that NE-SW faults become younger toward the oceanic domain controlling the crustal thinning which led to the onset of oceanic spreading. The third set of faults trends N-S and is related to the Limpopo FZ. Here, the inner SDRs are cross-cut by a major sub-vertical strike-slip fault. Finally, several Early Cretaceous faults reactivate older structures (*e.g.*, the Jurassic faults), in particular along the Naude Ridge (Fig. 2b).

4.2. The mantle plume hypothesis

The abundance of magmatism through ongoing extension in the Natal Valley (Fig. 2b) (*e.g.* inner and outer thick-SDRs, magmatic underplating…) implies particular thermal conditions in the area. The inferred huge volume of magma cannot be explained by a classic adiabatic melting process related to rifting. In addition, all our geochemical results are very consistent with most magmas being formed through melting of mantle sources with very primitive compositions as other well-documented CFB domains as well as most of the Karoo LIP (Fig. 6) (Turunen *et al*., 2019). All elements described before lead us to adhere to a plume hypothesis as suggested by some previous studies (*e.g.*, White & McKenzie, 1989; White, 1997; Storey & Kyle, 1997). Such a hypothesis is also consistent with previous works (*e.g.*, Larsen, 1990) suggesting that much wider SDRs are imaged near hot-spot trails. These latter are also probably caused by the thinning of the crust, which favors decompression in the underlying mantle, which in turn, increases melt localization and production (White & McKenzie, 1989; Berndt et al., 2001). In

any case, the impingement and influence of a mantle plume that may be responsible for such an abrupt continent to oceanic transition (see Fig. 3a) suggests a protracted thermal activity ranging from ca. 183 Ma to 165 – 160 Ma that also drove the Natal rifting. Such thermal impact on rift localization is consistent with previous numerical studies (*e.g.* Buck, 2004; Watremez *et al*., 2013).

4.3. Tectonic and lithospheric inheritance: a precursor to the break-up of Gondwana

Watkeys (2002) showed evidences of tectonic activity at least 70 m.y. before the arrival of the plume along the Limpopo Belt. Based on the seismic reflection profile along the eastern part of the south MCP, Roche *et al*. (2021) showed also N-S trending faults related to a Permo-Triassic event. This suggests that pre-existing structures influence the location of the future plume and rift. Further, various studies proposed a correlation between the trend of the faults and the nature of the basement (*e.g.*, Watkeys & Sokoutis, 1998; Roche *et al*., 2021). They showed that Permo-Triassic and Jurassic faulting in the Archean region (*i.e.,* in the Kaapvaal craton, Fig. 1b) displays N-S trending faults whereas faults in the region of Proterozoic basement display ENE-SWS trends. Following this interpretation, we suggest that Archean crust is mainly located along the proximal parts of the Mozambique coast whereas Proterozoic crust can be observed in the southern part of Zululand basin and in the Natal Valley (Fig. 1b). This hypothesis is also consistent with (i) our isotopic data showing that the compositions of samples from wells located next to the Lebombo Monocline and within the MCP (Zululand, Funhalouro and Nhachengue) are different from those located eastward such as Nhamura, and (ii) Moulin *et al*. (2020) who point to the resemblance between the MCP and the Kaapval craton through a comparison of their seismic data with these data from the Lebombo monocline (*e.g.*, Kwadiba *et al*., 2003). Therefore, the ascending plume-related material is probably channeled by the

presence of contrasting lithosphere age and rheology. Koptev *et al*. (2016) reported similar effects through high-resolution 3D thermo-mechanical numerical models in the Central East African Rift.

4.4. Geodynamic implications

We propose a simplified continental breakup model (Fig. 7) with regional implications (Fig. 8), the key features of which are summarized in Figure 9. The geodynamic boundary conditions are (i) the structural inheritance at lithospheric-scale, (ii) the high and sustained magmatic activity during the Early Jurassic (the Karoo LIP at ca. 183 Ma; Jourdan *et al*., 2007a; Svensen *et al*., 2012) to Middle Jurassic related to a mantle plume impingement below the Natal Valley (White & McKenzie, 1989; White, 1997; Storey & Kyle, 1997) and (iii) the migration of Antarctica with respect to Africa in two stages.

Early Jurassic rifting is localized in the Proterozoic domain between the two Archean African and Antarctica domains at around 180 Ma (Fig. 7a and T_2 stage, Figs. 8b and 9). Preexisting basement structures (T_1 stage, Fig. 8a and 9) thus likely favor the formation of the N-S and NE-SW basins filled by volcanic rocks. They both result from an oblique extension that is consistent with a NW-SE opening during several Myr (Figs. 7b and 7c). Although our observations do not allow us to estimate the age of oceanic spreading onset, the simplest interpretation is probably at around 160 Ma (Fig. 7d) as it is the case in the Angoche segment (Senkans *et al*., 2019). Indeed, both areas not only display the same geometry but also belong to the same geodynamic system. The presence of SDRs reveals that the formation of this magmatic crust may be rapid at the rift scale (few Myr, Sapin *et al*., 2021). In our interpretation, the continental rocks from the DSDP 249 may be a Precambrian continental fragment (similar to the Limpopia fragment, Reeves *et al*., 2016) that remained part of Antarctica (Fig. 8). Transfer faults zone along the

western side of the Dana and Galathea plateaus thus may have formed at ca. 160 Ma, whereas the eastern side was affected by the transform movement at ca. 156 Ma. Here, volcanic wedges related to the Limpopo transform fault activity may be locally preserved.

After 156 Ma (T_3 stage, Figs. 8c and 9), the Jurassic NE-SW trending basins were locally reactivated through a strike-slip faults system during the Cretaceous that was probably related to the right-lateral movement of the Agulhas FZ. This faulting was coeval to subsidence that started in the Early Cretaceous in the entire region (Baby *et al*., 2018), and might have been related to the decreasing influence of the mantle plume. The southern part of the Zululand basin, and especially the southern part of the Mozambique F.Z. then records an intense volcanic activity (Gohl *et al*., 2011; Fischer *et al*., 2016; Jacques *et al*., 2019). Although a correspondence with the Madagascar Province at 90 Ma cannot be totally excluded (*e.g.*, Storey *et al*., 1995; Bardintzeff *et al*., 2010), this LIP must have formed rapidly at around 130 Ma (Fischer *et al*., 2016) as the Agulhas Plateau (Gohl *et al*., 2011; Fischer *et al*., 2016). Such activity may be also related to the opening of the Weddell Sea.

ACKNOWLEDGMENTS

Vincent Roche was supported by a grant from the Pamela project. The PAMELA project (PAssive Margin Exploration Laboratories) is a scientific project led by Ifremer and TotalEnergies in collaboration with Université de Bretagne Occidentale, Université Rennes 1, Sorbonne Université, CNRS and IFPEN. We thank Captain Thierry Alix, the crews and the MCS technicians of the Pourquoi Pas? (IFREMER/GENAVIR). We also thank Jean-Claude Ringenbach at TotalEnergies for insightful assistance with seismic interpretations and Paul Perron at Sorbonne University chosen for his skills in the geo-referencing. We deeply thank F.

Corfu and an anonymous reviewer for both their assistance in improving this manuscript and the English style and grammar.

DATA AVAILABILITY STATEMENT

The data that support the findings of this study are available on request from the corresponding author. The data are not publicly available due to privacy or ethical restrictions.

SIGNIFICANCE STATEMENT

The Wilson cycle consists of plate tectonic processes where continents are fragmented, dispersed and then reassembled on the surface of Earth. One of the major challenges of the cycle is understanding the separation of continents that results in the birth and growth of a new oceans inducing the formation of passive margins. Results show that asthenospheric upwelling below South Mozambique control the rifting dynamics (*e.g.*, structural style and volume of magma) and the birth of the Natal Ocean at ca. 160 Ma.

REFERENCES

Baby, G., Guillocheau, F., Boulogne, C., Robin, C., & Dall'Asta, M. (2018). Uplift history of a transform continental margin revealed by the stratigraphic record: The case of the Agulhas transform margin along the Southern African Plateau. Tectonophysics, 731, 104-130. https://doi.org/10.1016/j.tecto.2018.03.014

Bardintzeff, J. M., Liégeois, J. P., Bonin, B., Bellon, H., & Rasamimanana, G. (2010). Madagascar volcanic provinces linked to the Gondwana break-up: Geochemical and isotopic evidences for contrasting mantle sources. Gondwana Research, 18(2-3), 295-314. https://doi.org/10.1016/j.gr.2009.11.010

Berndt, C., Mjelde, R., Planke, S., Shimamura, H., & Faleide, J. I. (2001). Controls on the tectono-magmatic evolution of a volcanic transform margin: the Vøring Transform

Margin, NE Atlantic. Marine Geophysical Researches, 22(3), 133-152. https://doi.org/10.1023/A:1012089532282

Bhattacharya, M., & Duval, G. (2016). A snapshot of the geotectonics and petroleum geology of the Durban and Zululand Basins, offshore South Africa. *First Break*, *34*(12). https://doi.org/10.3997/1365-2397.34.12.87303

Buck, W. (2004). Consequences of athenospheric variability on continental rifting, in Rheology and Deformation of the Lithosphere at Continental Margins, vol. 62, edited by G. D. Karner, B. Taylor, N. W. Driscoll, and D. L. Kohlstedt, pp. 1–30, Columbia Univ. Press.

Cox, K. G. (1992). Karoo igneous activity, and the early stages of the break-up of Gondwanaland. Geological Society, London, Special Publications, 68(1), 137-148. https://doi.org/10.1144/GSL.SP.1992.068.01.09

Cox, K.G. (1989). The role of mantle plumes in the development of continental drainage patterns. Nature 342, 873–877. https://doi.org/10.1038/342873a0

Dingle, R. V., & Scrutton, R. A. (1974). Continental breakup and the development of post-Paleozoic sedimentary basins around southern Africa. Geological Society of America Bulletin, 85(9), 1467-1474. https://doi.org/10.1130/0016-7606(1974)85<1467:CBATDO>2.0.CO;2

Eagles, G., & König, M. (2008). A model of plate kinematics in Gondwana breakup. Geophysical Journal International, 173(2), 703-717. https://doi.org/10.1111/j.1365-246X.2008.03753.x

Fischer, M. D., Uenzelmann-Neben, G., Jacques, G., & Werner, R. (2016). The Mozambique Ridge: a document of massive multi-stage magmatism. Geophysical Journal International, ggw403. https://doi.org/10.1093/gji/ggw403

Flores, G. (1984). The SE Africa triple junction and the drift of Madagascar. Journal of Petroleum Geology, 7(4), 403-418. https://doi.org/10.1111/j.1747-5457.1984.tb00885.x

Gale, N.H. A new method for extracting and purifying lead from difficult matrices for isotopic analysis, 1996, Analytica Chimica Acta, 332, 15-21

Gohl, K., Uenzelmann-Neben, G., & Grobys, N. (2011). Growth and dispersal of a southeast African large igneous province. South African Journal of Geology, 114(3-4), 379-386. https://doi.org/10.2113/gssajg.114.3-4.379

Goodlad, S. W. (1986). Tectonic and sedimentary history of the mid-Natal Valley (SW Indian Ocean) (Doctoral dissertation, University of Cape Town).

Green, A.G., 1972. Seafloor spreading in the Mozambique Channel. Nature Phys. Sci. 236, 19-21, 32.

Hanyu, T., Nogi, Y., & Fujii, M. (2017). Crustal formation and evolution processes in the Natal Valley and Mozambique Ridge, off South Africa. Polar Science, 13, 66-81. https://doi.org/10.1016/j.polar.2017.06.002

Heinonen, J.S., Carlson, R.W., Luttinen, A.V. (2010). Isotopic (Sr, Nd, Pb. and Os) composition of highly magnesian dikes of Vestfjella, western Dronning Maud Land, Antarctica: a key to the origins of the Jurassic Karoo large igneous province? Chem. Geol. 277 (3–4), 227–244.

Jacques, G., Hauff, F., Hoernle, K., Werner, R., Uenzelmann-Neben, G., Garbe-Schönberg, D., & Fischer, M. (2019). Nature and origin of the Mozambique Ridge, SW Indian Ocean. Chemical Geology, 507, 9-22. https://doi.org/10.1016/j.chemgeo.2018.12.027

Jourdan, F., Féraud, G., Bertrand, H., Watkeys, M. K., Kampunzu, A. B., & Le Gall, B. (2006). Basement control on dyke distribution in Large Igneous Provinces: case study of the Karoo triple junction. Earth and Planetary Science Letters, 241(1-2), 307-322. https://doi.org/10.1016/j.epsl.2005.10.003

Jourdan, F., Féraud, G., Bertrand, H., & Watkeys, M. K. (2007a). From flood basalts to the inception of oceanization: Example from the 40Ar/39Ar high-resolution picture of the Karoo large igneous province. Geochemistry, Geophysics, Geosystems, 8(2). https://doi.org/10.1029/2006GC001392

Jourdan, F., Bertrand, H., Schärer, U., Blichert-Toft, J., Féraud, G., & Kampunzu, A. B. (2007b). Major and trace element and Sr, Nd, Hf, and Pb isotope compositions of the Karoo large igneous province, Botswana–Zimbabwe: lithosphere vs mantle plume contribution. Journal of Petrology, 48(6), 1043-1077. https://doi.org/10.1093/petrology/egm010

Klimke, J., Franke, D., Mahanjane, E. S., & Leitchenkov, G. (2018). Tie points for Gondwana reconstructions from a structural interpretation of the Mozambique Basin, East Africa and the Riiser-Larsen Sea, Antarctica. Solid Earth, 9(1), 25-37. https://doi.org/10.5194/se-9-25-2018, 2018.

König, M., & Jokat, W. (2006). The Mesozoic breakup of the Weddell sea. Journal of Geophysical Research: Solid Earth, 111(B12). https://doi.org/10.1029/2005JB004035

König, M., & Jokat, W. (2010). Advanced insights into magmatism and volcanism of the Mozambique Ridge and Mozambique Basin in the view of new potential field data. Geophysical Journal International, 180(1), 158-180. https://doi.org/10.1111/j.1365-246X.2009.04433.x

Koptev, A., Burov, E., Calais, E., Leroy, S., Gerya, T., Guillou-Frottier, L., & Cloetingh, S. (2016). Contrasted continental rifting via plume-craton interaction: Applications to Central East African Rift, Geoscience Frontiers, 7(2), 221–236, doi:10.1016/j.gsf.2015.11.002.

Kwadiba, M. T. O. G., Wright, C., Kgaswane, E. M., Simon, R. E., & Nguuri, T. K. (2003). Pn arrivals and lateral variations of Moho geometry beneath the Kaapvaal craton. Lithos, 71(2-4), 393-411. https://doi.org/10.1016/j.lithos.2003.07.008

Larsen, H .C., (1990). Seismicr eflectionp rofiles acrosst he continentaml argin off East Greenland, in The Arctic Ocean Region, edited by A. Grantz, L. Johnsona, nd J.F. Sweeney, Geol. Soc. of Am., Boulder, Colo.

Leinweber, V. T., & Jokat, W. (2011). Is there continental crust underneath the northern Natal Valley and the Mozambique Coastal Plains?. Geophysical Research Letters, 38(14). https://doi.org/10.1016/j.tecto.2011.11.008

Leinweber, V. T., & Jokat, W. (2012). The Jurassic history of the Africa–Antarctica corridor—new constraints from magnetic data on the conjugate continental margins. Tectonophysics, 530, 87-101. https://doi.org/10.1029/2011GL047659

Leprêtre, A., Verrier, F., Schnurle, P., Evain, M., Aslanian, D., Leroy, S., de Clarens, P., Dias, N., Afilhado, A., Gonçalves, S. & Moulin, M. (2018). Insights on the crustal structure of the Natal Valley from combined wide-angle and reflection seismic data (MOZ3/5 cruise), South Mozambique Margin, SEISMIX Symposium,17 - 22 Juin 2018, Cracovie, Poland.

Leprêtre, A., Schnürle, P., Evain, M., Verrier, F., Moorcroft, D., De Clarens, P., ... & Moulin, M. (2021). Deep Structure of the North Natal Valley (Mozambique) Using Combined Wide-Angle and Reflection Seismic Data. Journal of Geophysical Research: Solid Earth, 126(4), e2020JB021171. https://doi.org/10.1029/2020JB021171

Li, H., Tang, Y., Moulin, M., Aslanian, D., Evain, M., Schnurle, P., ... & Li, J. (2021). Seismic evidence for crustal architecture and stratigraphy of the Limpopo Corridor: New insights into the evolution of the sheared margin offshore southern Mozambique. Marine Geology, 435, 106468. https://doi.org/10.1016/j.margeo.2021.106468

Mahanjane, E. S. (2012). A geotectonic history of the northern Mozambique Basin including the Beira High–a contribution for the understanding of its development. Marine and Petroleum Geology, 36(1), 1-12. https://doi.org/10.1016/j.marpetgeo.2012.05.007

Moulin, M., Aslanian, D., et al 2016a. PAMELA-MOZ03 cruise, RV Pourquoi pas ?, http://dx.doi.org/10.17600/16001600

Moulin, M., Aslanian, D., Evain, M., Leprêtre, A., Schnurle, P., Verrier, F., ... & PAMELA-MOZ35 Team. (2020). Gondwana breakup: messages from the North Natal Valley. Terra Nova. https://doi.org/10.1111/ter.12448

Moulin, M., Evain, M., et al. 2016b. PAMELA-MOZ05 cruise, RV Pourquoi pas ?, http://dx.doi.org/10.17600/16009500

Mueller, C. O. & Jokat, W. (2017). Geophysical evidence for the crustal variation and distribution of magmatism along the central coast of Mozambique. Tectonophysics, 712-713, 1-20, doi:10.1016/j.tecto.2017.06.007.

Mueller, C. O., & Jokat, W. (2019). The initial Gondwana break-up: a synthesis based on new potential field data of the Africa-Antarctica Corridor. Tectonophysics, 750, 301-328. https://doi.org/10.1016/j.tecto.2018.11.008

Planke, S., & Eldholm, O. (1994). Seismic response and construction of seaward dipping wedges of flood basalts: Vøring volcanic margin. Journal of Geophysical Research: Solid Earth, 99(B5), 9263-9278. https://doi.org/10.1029/94JB00468

Planke, S., Symonds, P. A., Alvestad, E., & Skogseid, J. (2000). Seismic volcanostratigraphy of large-volume basaltic extrusive complexes on rifted margins. Journal of Geophysical Research: Solid Earth, 105(B8), 19335-19351. https://doi.org/10.1029/1999JB900005

Ponte, J.-P. (2018). La marge africaine du canal du Mozambique, le système turbiditique du Zambèze : une approche « Source to Sink » au Méso – Cénozoïque. Sciences de la Terre. Université Rennes 1, 2018. Français. ⟨NNT : 2018REN1B005⟩. ⟨tel-01865479⟩

Ponte, J.-P., Robin, C., Guillocheau, F., Popescu, S., Suc, J.-P., Dall'Asta, M., Melinte-Dobrinescu, M. C., Bubik, M., Dupont, G., & Gaillot, J. (2019). The Zambezi delta (Mozambique channel, East Africa): High resolution dating combining bio-orbital and seismic stratigraphy to determine climate (palaeoprecipitation) and tectonic controls on a passive margin. Marine Petroleum Geology, 105, 293-310, doi:10.1016/j.marpetgeo.2018.07.017.

Raillard, S. (1990). Les marges de l'Afrique de l'Est et les zones de fractures associées: chaîne Davie et ride du Mozambique(Doctoral dissertation, Paris 6).

Reeves, C. V., Teasdale, J. P., & Mahanjane, E. S. (2016). Insight into the Eastern Margin of Africa from a new tectonic model of the Indian Ocean. Geological Society, London, Special Publications, 431(1), 299-322. https://doi.org/10.1144/SP431.12

Renne P.R., Balco G., Ludwig R.L., Mundil R., Min K., (2011). Response to the comment by W.H. Schwarz et al. on "Joint determination of ^{40}K decay constants and ^{40}Ar∗/^{40}K for the Fish Canyon sanidine standard, and improved accuracy for ^{40}Ar/^{39}Ar geochronology" by PR Renne et al. (2010). Geochimica Cosmochimica Acta, 75, 5097-5100.

Renne P.R., Mundil R., Balco G., Min K., Ludwig R.L., (2010). Joint determination of ^{40}K decay constants and ^{40}Ar∗/^{40}K for the Fish Canyon sanidine standard, and improved accuracy for ^{40}Ar/^{39}Ar geochronology. Gechimica Cosmochimica Acta, 74, 5349–5367.

Renne, P. R. et al. (1998). Intercalibration of standards, absolute ages and uncertainties in 40Ar/39Ar dating. Chem. Geol.145, 117–152.

Révillon, S., Jouet, G., Bayon, G., Rabineau, M., Dennielou, B., Hémond, C., Berné, S. (2011) The provenance of sediments in the Gulf of Lions, Western Mediterranean Sea. Geochemistry, Geophysics and Geosystems.

Riley, T. R., Millar, I. L., Watkeys, M. K., Curtis, M. L., Leat, P. T., Klausen, M. B., & Fanning, C. M. (2004). U–Pb zircon (SHRIMP) ages for the Lebombo rhyolites, South Africa: refining the duration of Karoo volcanism. Journal of the Geological Society, 161(4), 547-550. https://doi.org/10.1144/0016-764903-181

Roche, V., & Ringenbach, J. C. (2021). The Davie Fracture Zone: A recorder of continents drifts and kinematic changes. Tectonophysics, 229188. https://doi.org/10.1016/j.tecto.2021.229188

Roche, V., Leroy, S., Guillocheau, F., Revillon, S., Ruffet, G., Watremez, L., ... & Despinois, F. (2021). The Limpopo Magma-Rich Transform Margin, South Mozambique–2: Implications for the Gondwana Breakup. *Tectonics*, *40*(12), e2021TC006914. https://doi.org/10.1029/2021TC006915

Ruffet, G., Féraud, G., Amouric, M., 1991. Comparison of ^{40}Ar-^{39}Ar conventional and laser dating of biotites from the North Trégor Batholith. Geochimica Cosmochimica Acta 55, 1675–1688.

Ruffet, G., Féraud, G., Balèvre, M., Kiénast, J.-R., 1995. Plateau ages and excess argon in phengites: an ^{40}Ar-^{39}Ar laser probe study of Alpine micas (Sesia Zone, Western Alps, northern Italy). Chemical Geology 121, 327–343.

Ruffet, G., Gruau, G., Balèvre, M., Féraud, G., Philippot, P., 1997. Rb-Sr and ^{40}Ar-^{39}Ar laser probe dating of high-pressure phengites from the Sesia zone (Western Alps): underscoring of excess argon and new age constraints on the high-pressure metamorphism. Chemical Geology 141, 1–18.

Salman, G., & Abdula, I., 1995. Development of the Mozambique and Ruvuma sedimentary basins, offshore Mozambique. Sedimentary Geology, 96(1-2), 7-41, doi.org/10.1016/0037-0738(95)00125-R

Sandwell, D. T., & Smith, W. H. (2009). Global marine gravity from retracked Geosat and ERS-1 altimetry: Ridge segmentation versus spreading rate. Journal of Geophysical Research: Solid Earth, 114(B1). https://doi.org/10.1029/2008JB006008

Sapin, F., Ringenbach, J. C., & Clerc, C. (2021). Rifted margins classification and forcing parameters. Scientific Reports, 11(1), 1-17. https://doi.org/10.1038/s41598-021-87648-3

Senkans, A., Leroy, S., d'Acremont, E., Castilla, R., & Despinois, F. (2019). Polyphase rifting and break-up of the central Mozambique margin. Marine and Petroleum Geology, 100, 412-433. https://doi.org/10.1016/j.marpetgeo.2018.10.035

Storey, B. C., & Kyle, P. R. (1997). An active mantle mechanism for Gondwana breakup: Plumes, Plates and Mineralisation'97 Symposium. South African Journal of Geology, 100(4), 283-290.

Storey, M., Mahoney, J. J., Saunders, A. D., Duncan, R. A., Kelley, S. P., & Coffin, M. F. (1995). Timing of hot spot—related volcanism and the breakup of Madagascar and India. Science, 267(5199), 852-855. DOI: 10.1126/science.267.5199.852

Svensen, H., Corfu, F., Polteau, S., Hammer, Ø., & Planke, S. (2012). Rapid magma emplacement in the Karoo large igneous province. Earth and Planetary Science Letters, 325, 1-9. https://doi.org/10.1016/j.epsl.2012.01.015

Thompson, J. O., Moulin, M., Aslanian, D., De Clarens, P., & Guillocheau, F. (2019). New starting point for the Indian Ocean: Second phase of breakup for Gondwana. Earth-science reviews, 191, 26-56. https://doi.org/10.1016/j.earscirev.2019.01.018

Tikku, A. A., Marks, K. M., & Kovacs, L. C. (2002). An Early Cretaceous extinct spreading center in the northern Natal Valley. Tectonophysics, 347(1-3), 87-108. https://doi.org/10.1016/S0040-1951(01)00239-6

Turunen, S.T., Luttinen, A.V., Heinonen, J.S., Jamal, D.L. (2019). Luenha picrites, Central Mozambique – Messengers from a mantle plume source of Karoo continental flood basalts? Lithos 346–347, 105152. https://doi.org/10.1016/j.lithos.2019.105152

Watkeys, M. K. (2002). Development of the Lebombo rifted volcanic margin of southeast Africa. Special paper-Geological Society of America, (362), 27-46.

Watkeys, M. K., & Sokoutis, D. (1998). Transtension in southeastern Africa associated with Gondwana break-up. Geological Society, London, Special Publications, 135(1), 203-214. https://doi.org/10.1144/GSL.SP.1998.135.01.13

Watremez, L., Burov, E., d'Acremont, E., Leroy, S., Huet, B., Le Pourhiet, L., & Bellahsen, N. (2013). Buoyancy and localizing properties of continental mantle lithosphere: Insights from thermomechanical models of the eastern Gulf of Aden, Geochem. Geophys. Geosyst., 14(8), 2800–2817, doi:10.1002/ggge.20179.

Watremez, L., Leroy, S., d'Acremont, E., Roche, V., Evain, M., Leprêtre, A., ... & Moulin, M. (2021). The Limpopo Magma-Rich Transform Margin, South Mozambique: 1. Insights From Deep-Structure Seismic Imaging. Tectonics, 40(12), e2021TC006915. https://doi.org/10.1029/2021TC006914

White, R. S. (1997). Mantle plume origin for the Karoo and Ventersdorp flood basalts, South Africa. South African Journal of Geology, 100(4), 271-282. https://hdl.handle.net/10520/EJC-92973aa30

White, R., & McKenzie, D. (1989). Magmatism at rift zones: the generation of volcanic continental margins and flood basalts. Journal of Geophysical Research: Solid Earth, 94(B6), 7685-7729. https://doi.org/10.1029/JB094iB06p07685

White, W.M., Albaréde, F., Telouk, P. (2000). High-precision analysis of Pb isotope ratios by multi-collector ICP-MS. Chem.Geol. 167,257–270

FIGURE CAPTIONS

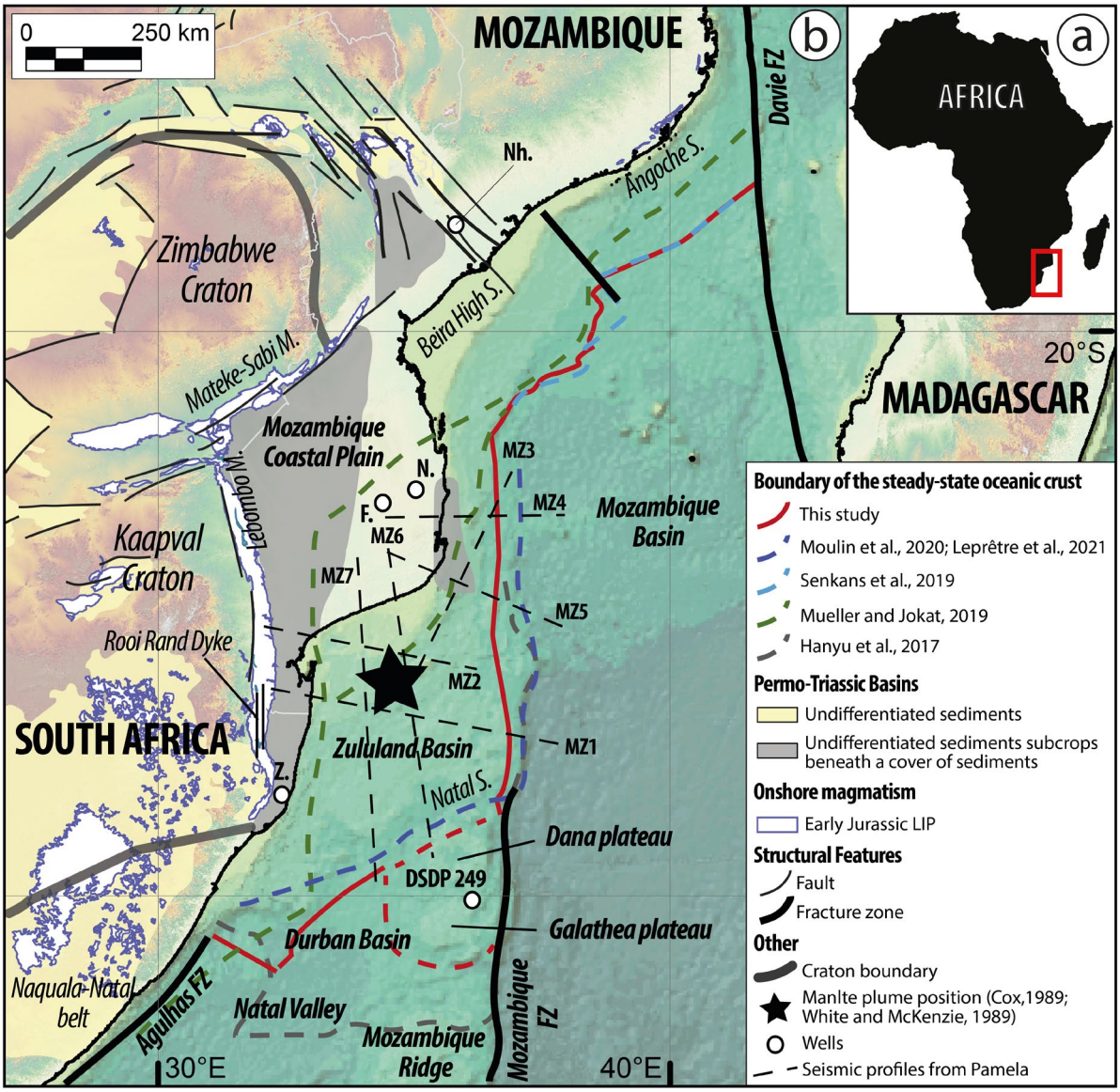

Figure 1: Location maps. (a) Red box in the top right corner shows the location of Fig. 1b. (b) Location map of the Mozambique-Natal area showing the main structures as the fracture zones and shear zones, and the distribution of Karoo Large Igneous Province (LIP) modified from Roche *et al*. (2021). Note that the Zululand and Durban basins are subdivided by the NE-SW trending Naude Ridge. F = Funhalouro, FZ = Fracture Zone, N = Nhachengue, Nh = Nhamura, M = Monocline, S = segment, Z = Zululand.

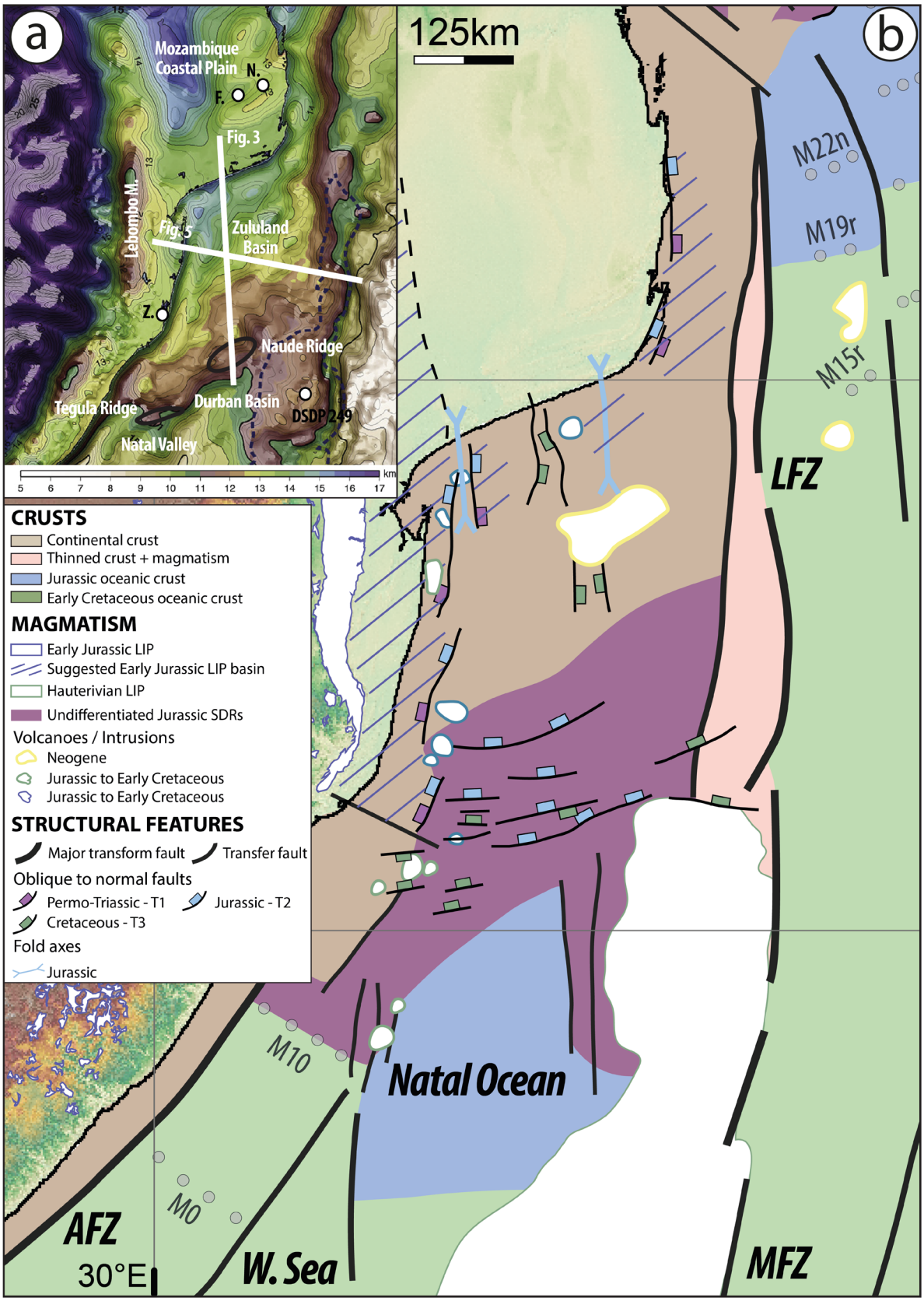

Figure 2: Overview of the study area. (a) Map modified from Hanyu *et al*. (2017) showing estimated crustal thicknesses in km based on gravity data. Well locations and the general cross-sections are indicated. Even though these values are smaller than the recently reported crustal thicknesses which were obtained by the wide-angle seismic method (Moulin *et al*., 2020; Leprêtre *et al*., 2021), the lower values in the Durban basin (10 km) fit well with our interpreted oceanic domain in Fig. 2b. Note that such a difference in the continental domain between the two methods may be explained by an underestimation of the basement density values in the gravity inversion method. The abbreviations are indicated in the previous figure. (b) Map showing simplified offshore crustal domains of the Natal area based on seismic observations, including previous observations from Roche *et al*. (2021) for the Limpopo transform segment. Small dots indicate magnetic anomalies identified by Goodlad *et al*. (1982) and Mueller and Jokat (2019). AFZ = Agulhas Fracture Zone; LIP = Large Igneous Province, LFZ = Limpopo Fracture Zone, MFZ = Mozambique Fracture Zone, SDRs = Seaward Dipping Reflectors, W = Weddell.

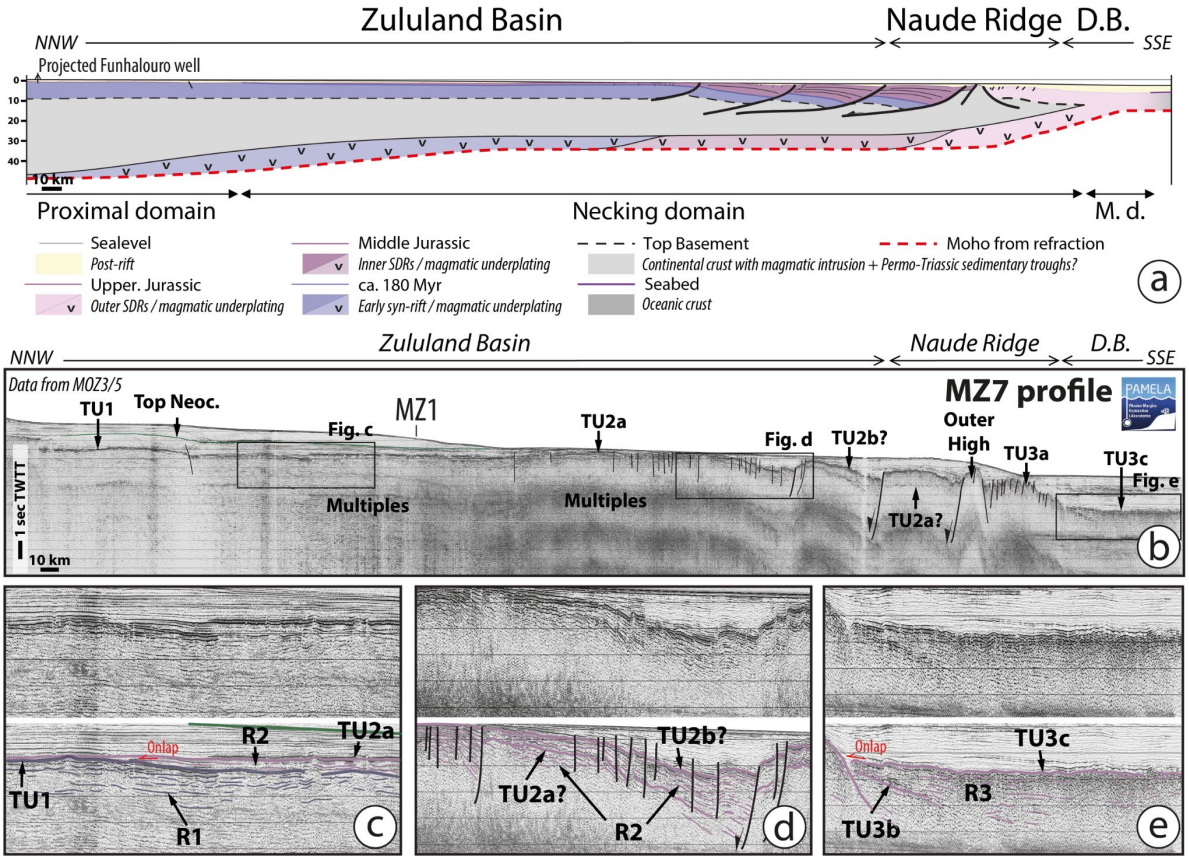

Figure 3: (a) Simplified interpretation of the combined MZ7 seismic profile and velocity model modified from Leprêtre *et al*. (*2021*). Note that oceanic crustal thickness in the southwards termination of the profile reaches approximatively 9 km and is thicker than normal oceanic crust suggesting that crust here is highly magmatic. Three domains are recognized: (i) the Proximal domain is mainly preserved onshore and it underwent modest stretching; (ii) the Necking domain corresponds to the onset of crustal thinning and inner SDRs to the limit of the continental crust; it is characterized by a proximal necking with a large basin of inner SDRs packages and a distal short necking (~ 60 km) that shows a radical thinning and outer SDRs; (iii) the Magmatic domain (M. d.) forms distal necking accommodated by magmatic additions (outer SDRs). Note that the horizon ca. 180 Myr is constrained by several wells (see main text). (b) Raw and interpreted Profile MZ7, modified from Leprêtre *et al*. (2021), corresponding to the previous cross-section. (c) Zoom showing relationships between TU1 and TU2a and R1 and R2. (d) Various set of inner SDRs (R3) controlled by NE-SW trending faults. These volcanic

sequences may be separated by nearly continuous reflectors tentatively labeled TU2a and TU2b. (e) Insert showing the most distal domain which is characterized by thick outer SDR packages (R3) thinning toward a classic oceanic crust. The data are courtesy of Pamela-MOZ03. D.B. = Durban Basin, Neoc. = Neocomian, TU = Top Unit, R = Reflectors.

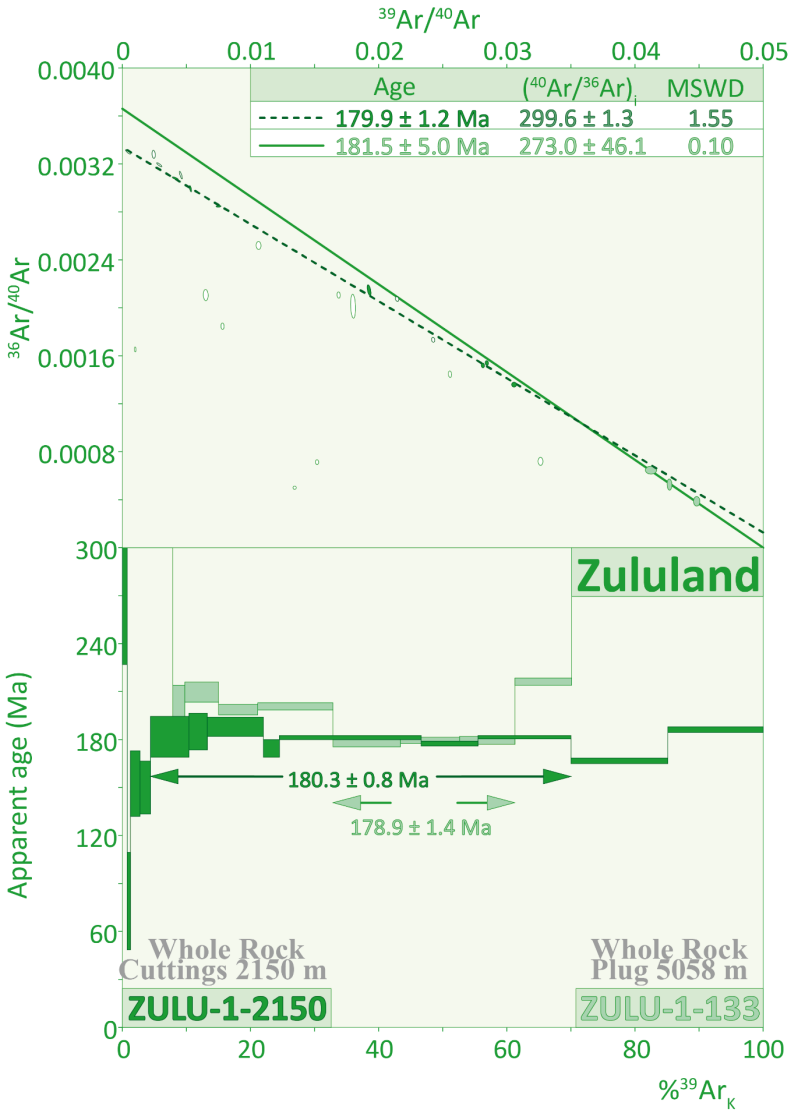

Figure 4: $^{40}Ar/^{39}Ar$ age spectra and inverse isochron ($^{36}Ar/^{40}Ar$ vs. $^{39}Ar/^{40}Ar$) diagrams of two mafic whole rock. Rock fragments collected from the Zulu-1-2150 cuttings and the Zulu-1-133 plug, both from the Zululand drill core. The isochrone calculations provide reliable parameters (($^{40}Ar/^{36}Ar)_i$ and MSWD) that allow the validation of isochrones ages, concordant with each

other and with the above-mentioned pseudo-plateau ages. Sample locations are indicated in Fig. 2a and detailed results are present in Supplementary Material (see Tables 1, 2 and 3). Apparent age error bars are at the 1σ level; errors in the J-parameter are not included. Pseudo-plateau and pseudo-isochron ages are given with 1σ uncertainties and include errors in the J-parameter.

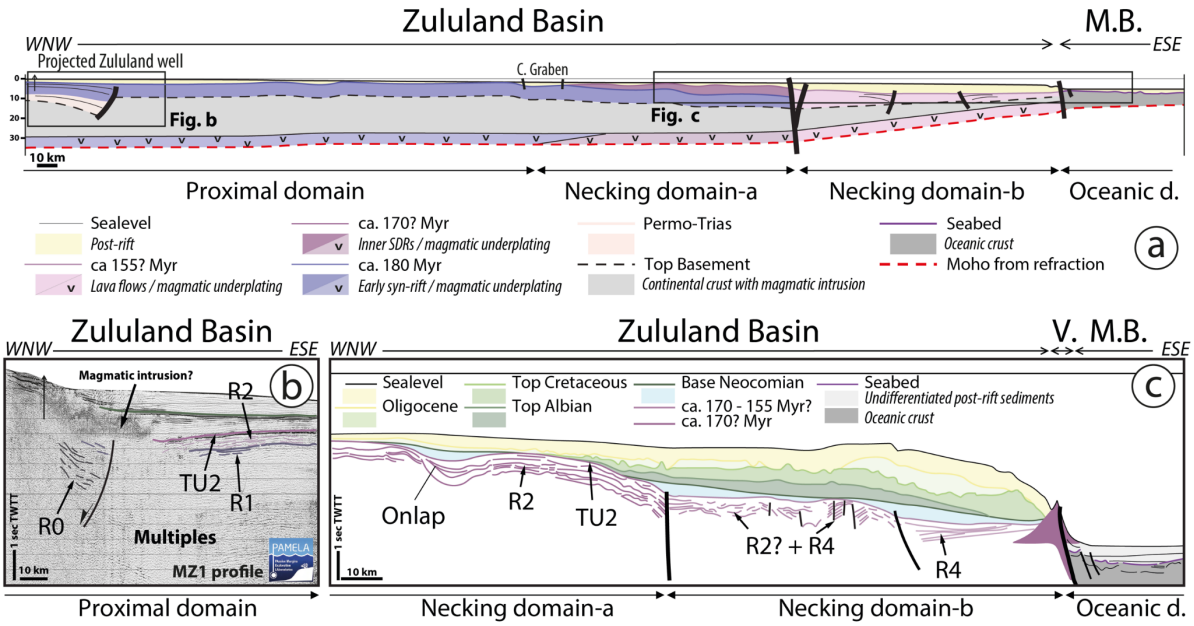

Figure 5: (a) Simplified interpretation based on several seismic profiles. Velocity model and Moho are from the MZ1 seismic profile from Moulin *et al.* (2020). This section is oblique to the previous one and cross-cuts the previous domains. The proximal domain is characterized by a thick pre-rift wedge made of a Permo-Triassic sedimentary trough and early syn-rift magmatic features related to the Karoo LIP (according to our new Argon ages). The first necking domain (Necking domain-a) corresponds to the thinning of the crust related to the rifted segment whereas the second one (Necking domain-b) is associated with the LFZ. This second necking shows a strong thinning of the continental crust and it is bounded by two major vertical strike-slip faults. In-between several intermediate faults may be observed controlling both seaward and landward dipping reflectors (see also Li *et al.*, 2021). The most distal domain corresponds to the oceanic crust. (b) Zoom of MZ1 seismic line showing the different groups

of reflectors, probably ranging from Permo-Triassic (R0) to Early Jurassic in age (R1 and R2). The data are courtesy of Pamela and more information can be found in Leprêtre *et al*. (2018). (c) Line drawing of MZ1 seismic line modified from Li *et al*. (2021) showing the main features across the eastern Natal margin. The necking domain-a show the inner SDRs (R2), characterized by several onlap and pinch out on deeper reflections. In the first kilometers, the necking domain-b shows discontinuous deep reflections attesting the existence of several minor vertical to sub-vertical faults. Reflectors located at the end of this domain have a wedge-shaped geometry and are interpreted as lava flows (R4). They are controlled by a fault implying magmatic infilling during the fault activity. D = Domain, M.B. = Mozambique Basin, TU = Top Unit, R = Reflectors, V = Volcano.

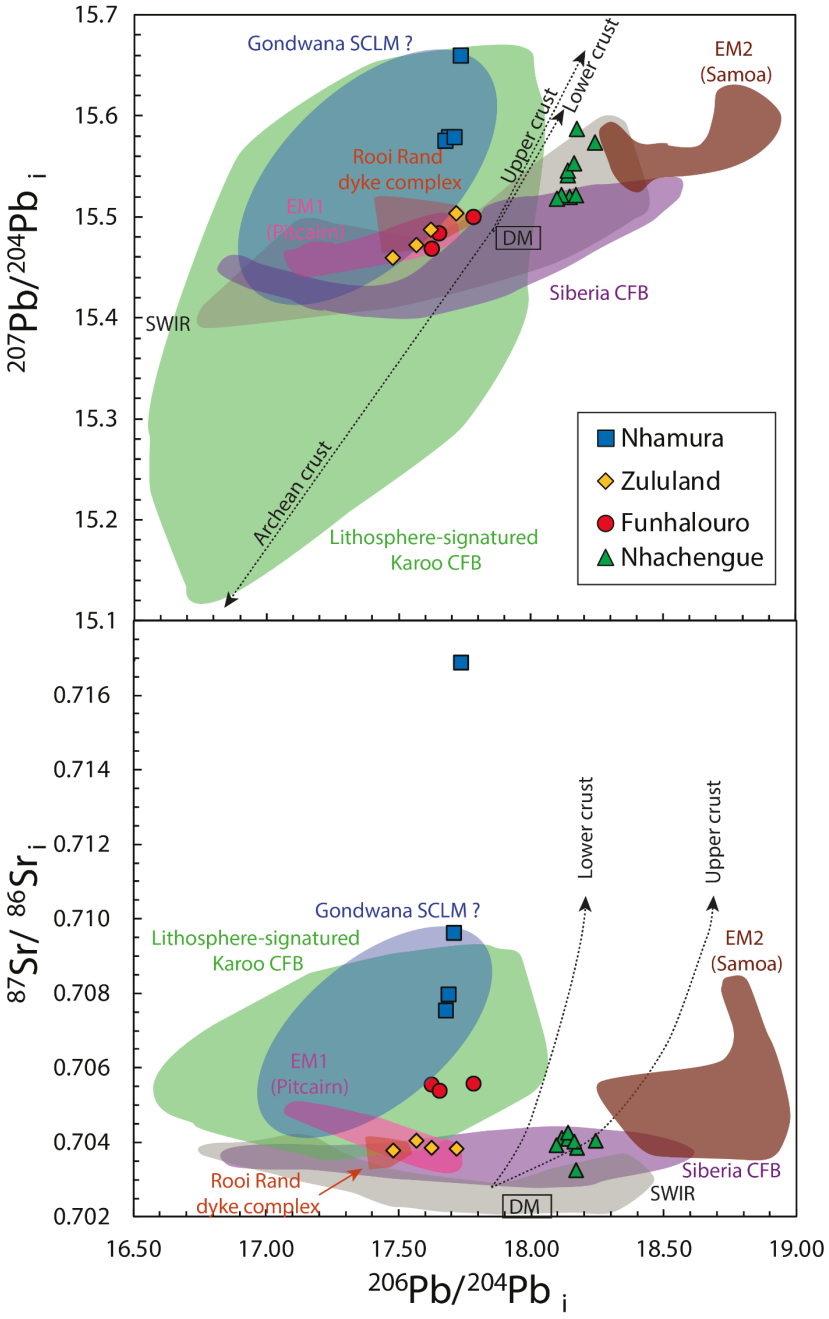

Figure 6: Initial $^{206}Pb/^{204}Pb$ versus initial $^{87}Sr/^{86}Sr$ and $^{207}Pb/^{204}Pb$ of basaltic samples and related volcanic rocks from Zululand, Funhalouro, Nhachengue and Nhamura wells as well as other Continental Flood Basalt (CFB) related fields and South West Indian Ridge (SWIR) samples. Detailed results are present in Supplementary Material (see Table 4). Initial isotope compositions were calculated at 180 Ma. Arrows represent assimilation-fractional crystallization (AFC) process involving Archean Crust, Upper Crust and Lower Crust as defined in Heinonen *et al*. (2010). Figure with source of data modified from Heinonen *et al*.

(2010). DM = depleted mantle; EM = enriched mantle components; SCLM = subcontinental lithospheric mantle.

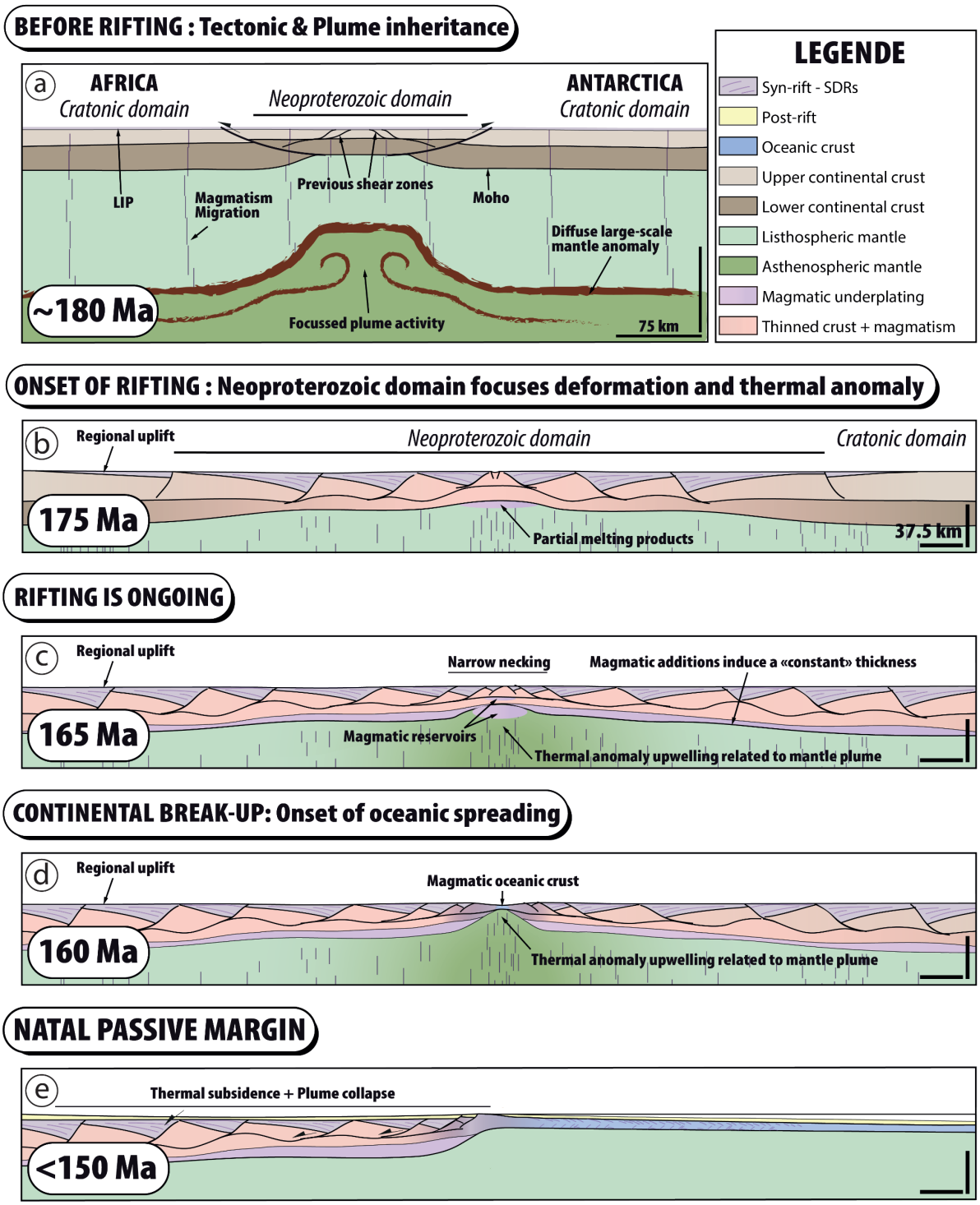

Figure 7: Conceptual model illustrating the tectonic evolution of the area consistent with data in a magma-rich setting. (a) Diffuse large-scale mantle temperature anomaly lead to vertical

melt transport with surface expression (LIP) and underplating across a broad region. (b) Mantle plume started to localize below the Natal valley, in-between both cratonic lithospheres. Extensive structures as high-angle normal faults may then be formed whereas volcanic activity is ongoing. The total extension is around 150 km compared to the previous cartoon. (c) Strong vertical thermal gradient related to the upwelling asthenosphere that induces several magmatic chambers within upper structural levels. The cumulated extension is around 200 km. (d) High thermal anomaly from focused mantle plume activity, weaks the crust, localizing and favoring initial burst of oceanic crust with a high degree of melting. (e) The extension has ceased in the South Natal area and seafloor oceanic spreading onset at chron M33.

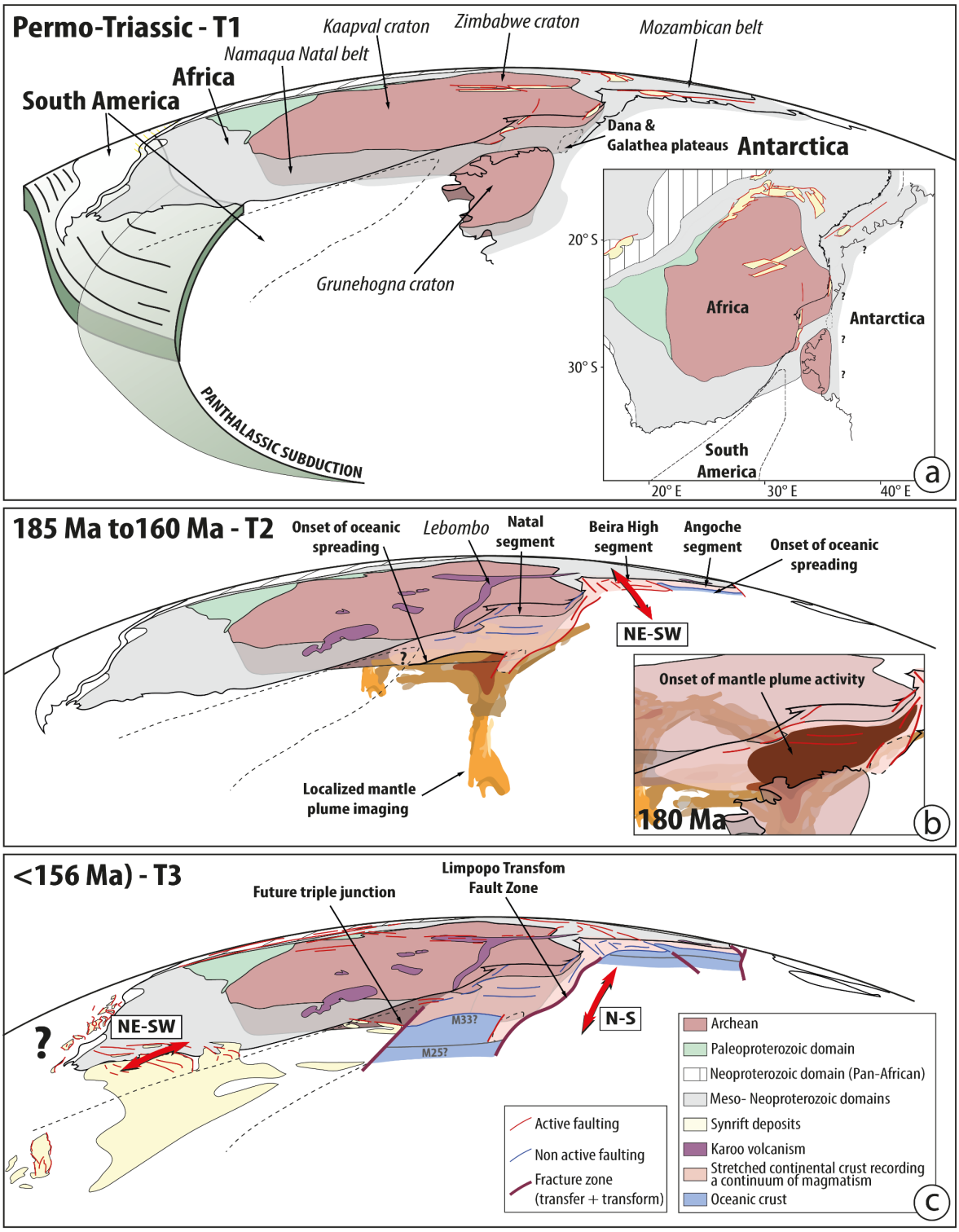

Figure 8: Simplified 3D geodynamic evolution of the southern Gondwana. (a) The Permo-Triassic period is characterized by localized rifts. (b) The beginning of the Karoo mantle plume and its tectonic interactions before and during the onset of oceanic spreading along the Angoche and Natal segments. Note also that mantle plume started to localize below the Zululand basin,

in-between the two cratonic lithospheres - *i.e.* in the Meso-Neoproterozoic domains showing a relevant structural inheritance. (c) Seafloor spreading is ongoing in the whole Mozambique area. The age of 156 Ma age corresponds to the onset of the Limpopo transform margin. The future plate triple junction leads to the dislocation of a part of Gondwana at around 130 Ma triggering the formation of the Weddell Sea and the Atlantic Ocean. The proposed Antarctica position is based on the craton location (see Fig. 8a), but the plate evolution of Antarctica through time is not shown. Abbreviations are indicated in previous Figs. 1 and 2.

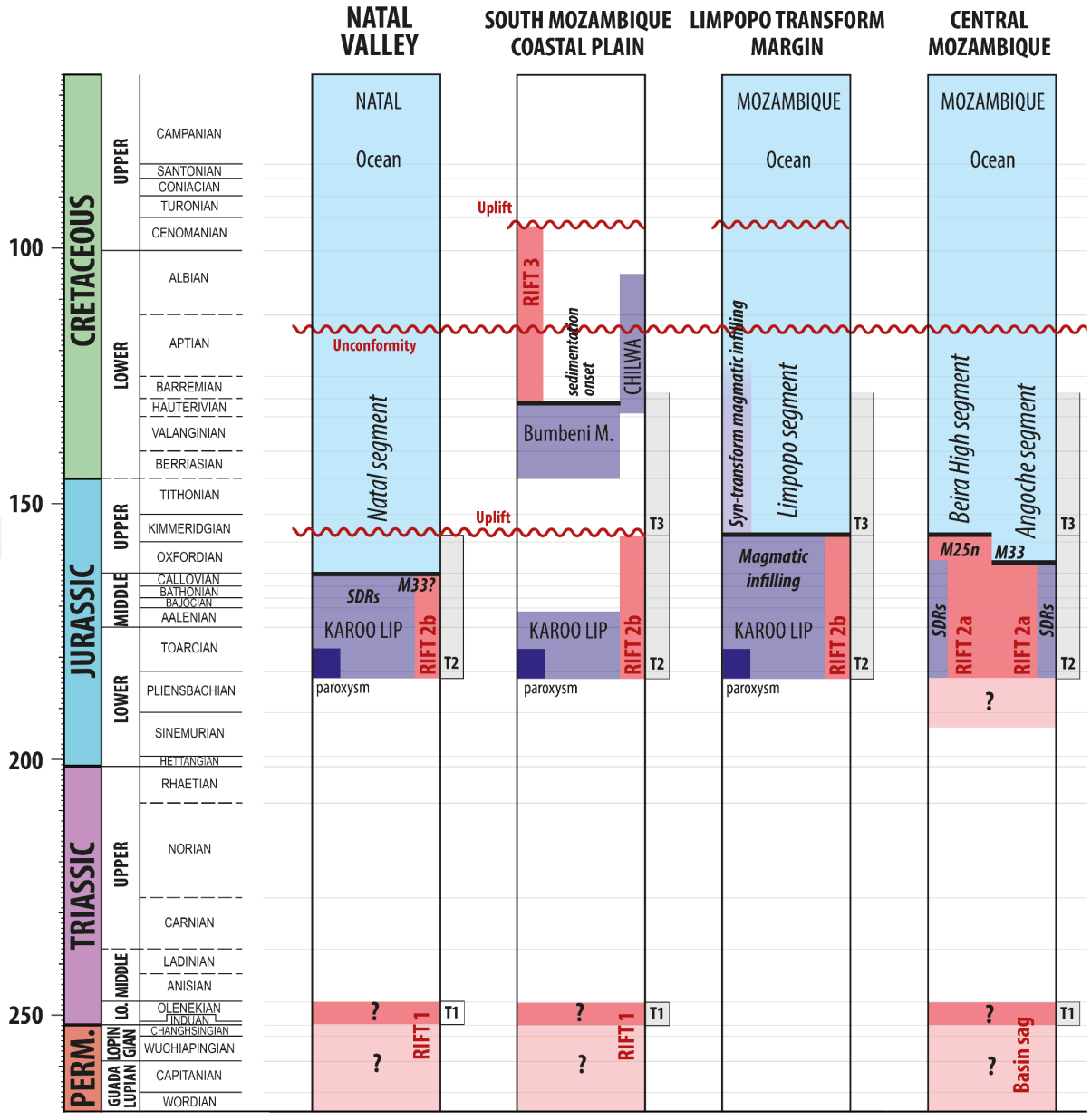

Figure 9: Simplified geodynamic chart modified from Roche *et al*. (2021). The violet color represents the magmatic systems. The red color represents a rifting period. Rift2a is an orthogonal rifting. Rift2b is oblique to hyper-oblique rifting. Note that Permo-Triassic aborted rifts existing along the south Mozambican coast may be present in the Natal area. The blue color represents the ocean marked by the onset of oceanic spreading. Uplifts and unconformity are fully described in Ponte *et al*. (2018; 2019) and Baby *et al*. (2018) and briefly in this study. Abbreviations are indicated in previous Figs. 1 and 2. M = Movene.